



# Evolution of spectral and transport quantities with doping in the $SU(2)$ theory of cuprates

Corentin Morice, Xavier Montiel, Catherine Pépin

## ► To cite this version:

Corentin Morice, Xavier Montiel, Catherine Pépin. Evolution of spectral and transport quantities with doping in the  $SU(2)$  theory of cuprates. 2017. cea-01567560v1

**HAL Id: cea-01567560**

**<https://cea.hal.science/cea-01567560v1>**

Preprint submitted on 24 Jul 2017 (v1), last revised 18 Oct 2022 (v2)

**HAL** is a multi-disciplinary open access archive for the deposit and dissemination of scientific research documents, whether they are published or not. The documents may come from teaching and research institutions in France or abroad, or from public or private research centers.

L'archive ouverte pluridisciplinaire **HAL**, est destinée au dépôt et à la diffusion de documents scientifiques de niveau recherche, publiés ou non, émanant des établissements d'enseignement et de recherche français ou étrangers, des laboratoires publics ou privés.

# Evolution of spectral and transport quantities with doping in the SU(2) theory of cuprates

C. Morice,<sup>1</sup> X. Montiel,<sup>2</sup> and C. Pépin<sup>1</sup>

<sup>1</sup>*Institut de Physique Théorique, CEA, Université Paris-Saclay, Saclay, France*

<sup>2</sup>*Department of Physics, Royal Holloway, University of London, Egham, Surrey, United Kingdom*

(Dated: April 24, 2017)

Recent transport experiments in the cuprate superconductors linked the opening of the pseudogap to a change in electronic dispersion [S. Badoux et al., Nature 531, 210 (2015)]. Transport measurements showed that the carrier density sharply changes from  $x$  to  $1+x$  at the pseudogap critical doping, in accordance with the change from Fermi arcs at low doping to a large hole Fermi surface at high doping. The SU(2) theory of cuprates shows that antiferromagnetic short range interactions cause the arising of both charge and superconducting orders, which are related by an SU(2) symmetry. The fluctuations associated with this symmetry form a pseudogap phase. Here we derive the renormalised electronic propagator under the SU(2) dome, and calculate the spectral functions and transport quantities of the renormalised bands. We show that their evolution with doping matches both spectral and transport measurements.

*Introduction* — Two of the most striking features of cuprate superconductors are their enigmatic pseudogap phase [1, 2] and how they evolve from a Mott insulator to a correlated metal with doping. Both features have been widely studied during the last thirty years [3–12] and many scenarii have been proposed to explain the physics of cuprate superconductors, based on antiferromagnetic fluctuations [3, 13, 14], strong correlations [5, 15, 16], loop currents [17, 18], emergent symmetry models [19, 20] and particle-hole patches [21, 22].

Recent transport experiments at high magnetic field in YBCO [23], Nd-LSCO [24] and LSCO [25] showed that these two features are intrinsically linked. Hall coefficient and resistivity measurements indeed yielded a sharp change of the carrier density at the pseudogap critical doping  $x^*$ , from  $x$  at low doping to  $1+x$  at high doping [23–25]. Resolving the difference between this critical doping and others, such as the one corresponding to the Fermi surface reconstruction caused by the arising of the charge density wave phase, was made possible by the use of samples with adjacent dopings [23–26].

At low doping ( $x < x^*$ ), this change in carrier density is consistent with ARPES experiments which show small Fermi arcs corresponding to  $x$  carriers per unit cell [27]. At high doping ( $x > x^*$ ), the carrier density dependence is in agreement with the quantum oscillation measurements which find a large hole Fermi-surface enclosing a  $1+x$  volume, in agreement with band structure calculations [28, 29].

Several models have been suggested to explain this change in the carrier density. Some are based on strong coupling or topological order [30], which give small Fermi pockets at low temperature which enlarge when temperature rises. Other are based on long-range fluctuations, either superconducting [31, 32], antiferromagnetic [33–35], or related to a charge density wave order [36] which yield a large Fermi surface gapped at low temperature. Here we discuss a theory related to the second category, where the fluctuations ensue from the emergence of an

SU(2) symmetry between the charge and superconducting operators [22].

In this letter, we study electronic transport and spectral functions in the SU(2) theory for cuprate superconductors. We first derive the electron propagator in the pseudogap phase, and then use it to calculate resistivity, Hall resistivity, and spectral functions. Our results agree with both spectral [37] and transport [23] measurements.

*SU(2) theory* — The short-range antiferromagnetic model ( $t$ - $J$ ), widely studied in the context of high-temperature superconductivity [5], was recently used as the basis of a theory of the pseudogap [22]. Decoupling the antiferromagnetic interaction term in the charge and superconducting channels yields two corresponding order parameters. In the strong coupling (large  $J$ ) limit, these two order parameters were shown to be related by an exact SU(2) symmetry on a line of the Brillouin zone which goes through the hot spots. This generalises some earlier work derived from the spin-fermion model and limited to the hot spots [38]. The conservation of this SU(2) symmetry leads to fluctuations, whose interaction with the fermions opens a gap in the antinodal region of the Brillouin zone. It is important to note that this derivation does not rely on the presence of a quantum critical point in the phase diagram of the cuprates. This SU(2) theory of the pseudogap has been shown to elucidate many characteristics of the cuprate superconductors, including Raman scattering [39], fixed-doping ARPES [40] and inelastic neutron scattering [41] responses, as well as the strange metal behaviour [22].

The composite order parameter corresponding to this SU(2) order is a  $2 \times 2$  matrix:

$$b \begin{pmatrix} \chi & \Delta \\ -\Delta^* & \chi^* \end{pmatrix} \text{ where } |\chi|^2 + |\Delta|^2 = 1$$

with  $\chi$  the charge order parameter,  $\Delta$  the superconducting order parameter and  $b$  the SU(2) phase [22]. Note that this order parameter is intrinsically not abelian. It is SU(2)-symmetric, meaning that there exists a set of op-

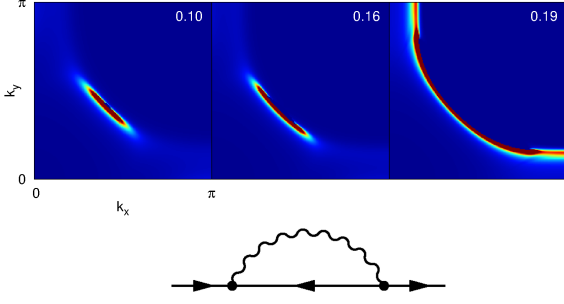


FIG. 1: Top: evolution of the spectral functions at zero frequency with doping. Note that because the renormalised bands are symmetrical with respect to zero energy, both spectral functions are equal at zero frequency. We therefore only plot one of them. Bottom: self-energy diagram for the renormalisation of the fermionic propagator. The straight lines are bare electron lines, while the wiggly line is the SU(2) fluctuations line.

erators forming an SU(2) algebra under which this composite order parameter is invariant [22].

*Derivation of the self-energy* — Expanding the action of the short range antiferromagnetic model linearly for small SU(2) fluctuations, one obtains an effective non-linear  $\sigma$ -model [22]. The effective action for the electrons is obtained by integrating out the SU(2) fluctuations in this model [22]:

$$S_{fin} = -\frac{1}{2} \text{Tr} \sum_{k,k',q,q',\sigma,\sigma'} \sigma\sigma' \langle \Delta_{kq}^\dagger \Delta_{k'q'} \rangle_Q \times \psi_{k+q,\sigma}^\dagger \psi_{-k+q,\bar{\sigma}}^\dagger \psi_{-k'+q',\bar{\sigma}'} \psi_{k'+q',\sigma'} \quad (1)$$

where  $k, k', q$  and  $q'$  are combined momentum and frequency indices,  $\sigma$  and  $\sigma'$  are spin indices and  $\psi^\dagger$  is the electron creation operator. One can simplify [22]:

$$\langle \Delta_{kq}^\dagger \Delta_{k'q'} \rangle_Q = \delta_{\mathbf{q},\mathbf{q}'} \pi_{kk'q}^s \quad (2)$$

where  $\pi_{kk'q}^s$  is the SU(2) fluctuations propagator:

$$\pi_{kk'q}^s = M_{0,k} M_{0,k'} \frac{\pi_0}{J_0 \epsilon^2 + J_1 (\mathbf{v} \cdot \mathbf{q})^2 - a_0} \quad (3)$$

where  $q = (\mathbf{q}, \epsilon)$ ,  $\pi_0$ ,  $J_0$  and  $J_1$  are coefficients,  $\mathbf{v}$  is the Fermi velocity, and  $a_0$  is a mass term. Inputting this in equation (1) gives the expression for the self energy:

$$-\Sigma(k) = \frac{1}{2} \sum_{q,\sigma} \pi_{kkq}^s G_{-k+q,\bar{\sigma}}^0 \quad (4)$$

where  $G^0$  is the free electron propagator. This self-energy corresponds to the diagram in figure 1. Approximating the sum by its low momentum and frequency contribution yields:

$$\Sigma(\mathbf{k}, \omega) = B \frac{M_{0,k}^2}{i\omega + \xi_{\mathbf{k}}} \quad (5)$$

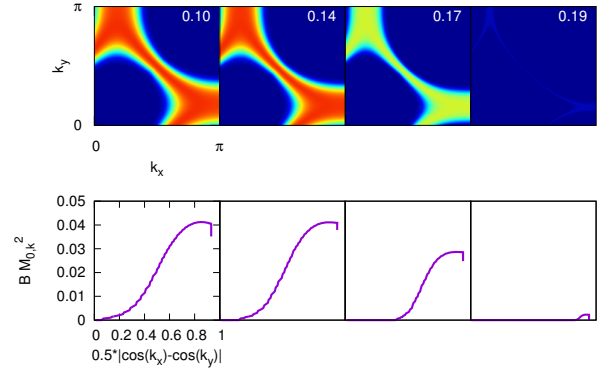


FIG. 2: Top: evolution of the gap  $BM_{0,k}^2$  with doping in a quarter of the Brillouin zone. The color blue is for zero. Bottom: gap on the Fermi surface with respect to the  $d$ -wave factor. A pure  $d$ -wave gap would be strictly linear.

where  $B$  is a parameter,  $k = (\mathbf{k}, \omega)$  and  $\xi_{\mathbf{k}}$  is the free electron dispersion. The renormalised electronic propagator therefore is:

$$G(\mathbf{k}, \omega) = \frac{1}{\omega - \xi_{\mathbf{k}} - B \frac{M_{0,k}^2}{\omega + \xi_{\mathbf{k}}}} \quad (6)$$

Let us note that this is very close to the form obtained in simpler forms of the SU(2) theory [39], the main difference being that in the latter case the denominator of the self-energy is  $\omega - \xi_{2p_{F(k)}}$ , where  $p_{F(k)}$  is a wave vector dependent ordering vector. Close to the Fermi surface,  $\xi_{2p_{F(k)}} \simeq -\xi_{\mathbf{k}}$ , which makes these two models consistent.

*Methods* — Separating the renormalised propagator (equation (6)) in simple elements gives us the expressions for the renormalised bands:

$$E^\pm(\mathbf{k}) = \pm \sqrt{\xi(\mathbf{k}, x)^2 + BM_{0,k}^2} \quad (7)$$

and corresponding spectral functions:

$$A^\pm(\mathbf{k}, \omega) = \frac{1}{\pi} \frac{W^\pm(\mathbf{k}) \Gamma^\pm(\mathbf{k})}{(\omega - E^\pm(\mathbf{k}, x))^2 + \Gamma^\pm(\mathbf{k})^2} \quad (8)$$

where the spectral weights are given by:

$$W^\pm(\mathbf{k}) = \frac{1}{2} \left( 1 \pm \frac{\xi(\mathbf{k}, x)}{\sqrt{\xi(\mathbf{k}, x)^2 + BM_{0,k}^2}} \right) \quad (9)$$

and  $\Gamma^\pm$  is the scattering rate of each renormalised band. We follow previous works [34, 42, 43] and neglect the scattering between the two renormalised bands. The longitudinal and transverse resistivities are given by [42]:

$$\sigma_{xx}^\pm = -\frac{2\pi e^2}{VN} \sum_{\mathbf{k}} (v_x^\pm(\mathbf{k}))^2 \int d\omega \frac{\partial f(\omega)}{\partial \omega} A^\pm(\mathbf{k}, \omega)^2 \quad (10)$$

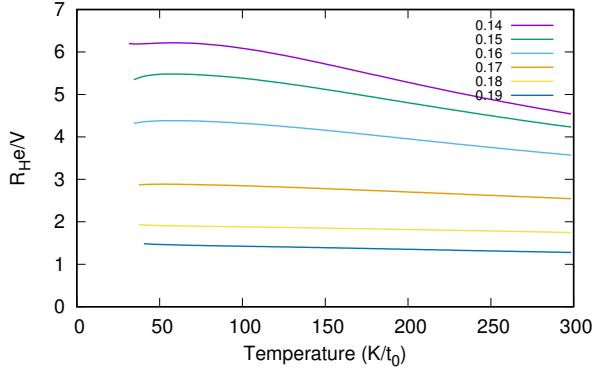


FIG. 3: Hall resistance in volume units with respect to temperature in Kelvin per units of  $t_0$ , for a range of hole dopings.

$$\sigma_{xy}^{\pm} = \frac{4\pi^2 e^3}{3VN} \sum_{\mathbf{k}} v_x^{\pm}(\mathbf{k}) \left( v_x^{\pm}(\mathbf{k}) \frac{\partial v_y^{\pm}(\mathbf{k})}{\partial k_y} - v_y^{\pm}(\mathbf{k}) \frac{\partial v_x^{\pm}(\mathbf{k})}{\partial k_x} \right) \times \int d\omega \frac{\partial f(\omega)}{\partial \omega} A^{\pm}(\mathbf{k}, \omega)^3 \quad (11)$$

The integral over frequency can be simplified using the standard approximation [44]:

$$\int_{-\infty}^{\infty} d\omega \left( \frac{\Gamma^{\pm}(\mathbf{k})}{(\omega - E^{\pm}(\mathbf{k}))^2 + \Gamma^{\pm}(\mathbf{k})^2} \right)^2 = \frac{\pi}{2} \frac{1}{\Gamma^{\pm}(\mathbf{k})} \quad (12)$$

which gives:

$$\sigma_{xx}^{\pm} = \frac{e^2}{VN} \sum_{\mathbf{k}} (v_x^{\pm}(\mathbf{k}))^2 \frac{W^{\pm}(\mathbf{k})^2}{\Gamma^{\pm}(\mathbf{k})} \frac{\beta e^{\beta E^{\pm}(\mathbf{k})}}{(e^{\beta E^{\pm}(\mathbf{k})} + 1)^2} \quad (13)$$

We generalise this approach to the cubic case and obtain:

$$\sigma_{xy}^{\pm} = -\frac{e^3}{2VN} \sum_{\mathbf{k}} v_x^{\pm}(\mathbf{k}) \left( v_x^{\pm}(\mathbf{k}) \frac{\partial v_y^{\pm}(\mathbf{k})}{\partial k_y} - v_y^{\pm}(\mathbf{k}) \frac{\partial v_x^{\pm}(\mathbf{k})}{\partial k_x} \right) \times \frac{W^{\pm}(\mathbf{k})^3}{\Gamma^{\pm}(\mathbf{k})^2} \frac{\beta e^{\beta E^{\pm}(\mathbf{k})}}{(e^{\beta E^{\pm}(\mathbf{k})} + 1)^2} \quad (14)$$

These expressions allow us to calculate the Hall resistance [42]

$$R_H = \frac{\sigma_{xy}^{+} + \sigma_{xy}^{-}}{(\sigma_{xx}^{+} + \sigma_{xx}^{-})^2} \quad (15)$$

We parametrize the symmetry breaking coefficient in the free energy using a smooth step function:

$$M_0^2 = \frac{1}{e^{30 * \left( \frac{\Delta \xi_{\mathbf{k}}}{\Delta_{SU2}} \right)^2 - 0.02} + 1} \quad (16)$$

where  $\Delta_{SU2}$  is the magnitude of the gap and  $\Delta \xi_{\mathbf{k}} = \frac{1}{2}(\xi_{\mathbf{k}} - \xi_{\mathbf{k}+\mathbf{Q}})$  is the SU(2) symmetry-breaking dispersion, or SU(2) line. The SU(2) wave vector  $Q_0$  is chosen

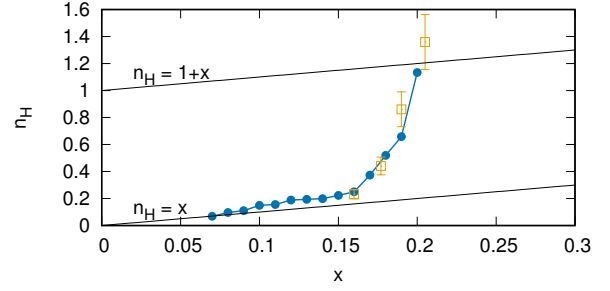


FIG. 4: Hall number with respect to doping (blue). The experimental values from [23] (orange) and the low-doping and high-doping asymptotes (black) are also plotted for reference. Note that  $x^* = 0.2$ .

as the vector between the two closest hot spots, following previous studies [22]. We set  $M_0$  to zero when smaller than one hundredth. If  $\Delta \xi_{\mathbf{k}}$  is zero, the SU(2) symmetry is conserved,  $M_0^2 = 1$ , and hence the gap is open. Conversely, if the SU(2) symmetry is broken,  $\Delta \xi_{\mathbf{k}}$  is finite, and the gap is small. This is consistent with the fact that the SU(2) fluctuations can only be strong if this symmetry is not broken. The  $\Delta_{SU2}$  parameter represents the magnitude of the pseudogap order parameter in the SU(2) theory and was parametrised by:

$$\Delta_{SU2} = \left( \frac{1}{e^{(x-0.175) \times 170} + 1} - 0.018 \right) \times 0.58 \quad (17)$$

For consistency we also set  $B = \Delta_{SU2}$ . We use  $\Gamma^{\pm} = 0.01 \times t_0$ , and set  $x^* = 0.2$ . We use the electronic dispersion used in a previous work [34], and shown to properly replicate the doping dependence of the Hall number for  $x > x^*$ .

**Results** — We calculated the magnitude of the gap  $B \times M_0^2$  over the Brillouin zone and on the Fermi surface (Figure 2). The gap opens along the SU(2) line, as found previously [22]. The SU(2) line crosses the Fermi surface at the hot spots, consequently of our choice of ordering wave-vector. The gap opens in the antinodal zone and is closed in the nodal zone. It gets both thinner and smaller in magnitude with rising doping and finally vanishes at the critical doping. This can be compared with ARPES data which showed that the pseudogap was closed in the nodal zone [37]. Our data fits qualitatively these experimental results, unlike methods based on a pure  $d$ -wave gap (i.e. a gap linear in the  $d$ -wave factor).

The spectral functions of the two renormalised bands at zero frequency were calculated using equation (8) (Figure 1). The dispersion in the denominator of the self-energy (equation (4)), which corresponds to the dispersion of the SU(2) fluctuations bosonic mode, is the opposite of the bare electronic dispersion. The self-energy therefore diverges on the Fermi surface. This also means that the renormalised bands are equal to each other up to a sign, and therefore the spectral functions at zero frequency are equal. Consequently, we only plot one of

them. The absence of gap in the nodal region causes the formation of a Fermi arc around the nodal point. This Fermi arc gets larger with larger doping, until it forms the whole Fermi surface at the critical doping  $x^*$ . The gap remains open at the hot spots for  $x < x^*$ , and closes close to the Brillouin zone edge slightly before (see Supplemental Material).

Using equations (13) and (14), we calculated the evolution of the Hall resistivity with temperature (Figure 3). For each doping, the Hall resistivity rises with decreasing temperature and saturates at low temperature. This rise is lower for higher dopings, and almost absent close to the critical doping. Note that the calculation does not reach absolute zero. This is due to the exponentials in the expressions for resistivities growing larger than the computational maximum. The zero-temperature Hall number  $n_H = V/eR_H$  (Figure 4) sharply changes from  $x$  to  $1 + x$  close to the critical doping, in agreement with experimental measurements on YBCO [23] and Nd-LSCO [24].

We compared these results to using a pure  $d$ -wave gap such as the one used in previous studies [34]. Naturally, because the dispersion of the bosonic mode is equal to minus the electronic dispersion, the gap opens everywhere but at the nodal points. Therefore the Hall resistance diverges at low temperature (see Supplemental Material). However one can measure the evolution of finite temperature values of the Hall resistance with doping. Interestingly, this displays a transition from  $x$  to  $1 + x$ , in fine agreement with experiments (see Supplemental Material).

*Discussion* — Our calculation of the evolution of the gap on the Fermi surface with doping closely resembles ARPES data [37] (Figure 1). Indeed, measurement of the photoemission gap above  $T_c$  found that a  $d$ -wave dependence could not describe what was seen experimentally: the gap is measured to be zero for a segment of the  $d$ -wave factor which grows with doping, unlike a  $d$ -wave gap which would be linear here. Experimental data then finds a close-to-linear increase in the gap, followed by a saturation at intermediate dopings [37]. Our data satisfactorily fits experimental data at low and intermediate doping. Indeed the saturation is not observed in the sample with the lowest doping, but data points for a  $d$ -wave factor larger than 0.8 have larger error bars and could fit a saturation, knowing that this is precisely the  $d$ -wave factor where we find a saturation. At high doping however, we find a segment for which the gap is zero which is much larger than in experiments. But this part of the experimental data is more noisy and closer to zero which makes us think that this could be due to experimental difficulties. Indeed, this observation is in contradiction with the length of the Fermi arc measured with ARPES, which can be seen to be large in other studies when plotted on the Brillouin zone [27], while the pseudogap is finite for a  $d$ -wave factor as low as 0.5. Finally, the strength of the gap at its maximum was measured to be about 50 meV at low doping, 40 meV at intermediate doping and

20 meV a high doping [37]. Our calculations reproduce this trend, although the sharp drop of this maximum at high doping has yet to be compared with experiments very close to the critical doping. We therefore conclude that our calculations are in agreement with  $d$ -wave-factor resolved ARPES data [37].

Our calculations therefore yield the arising of Fermi arcs, not Fermi pockets, in the pseudogap phase. This seems to be in contradiction with the Luttinger sum rule, which states that the volume of the Fermi surface is equal to the number of carriers. Indeed, here this volume is ill defined, since parts of its boundary have vanished. However the case of fluctuations gapping the Fermi surface is specific and has been treated in the preformed pairs model [31]. It was found that in this case the Luttinger sum rule is satisfied for the free fermions bands. Our situation is similar, except for the fact that phase fluctuations are replaced with SU(2) fluctuations.

The Hall number is a measurement of the number of carriers, and accordingly we find that the length of the Fermi arcs has a similar evolution to it. This also means that in order for the Hall number to reach the  $1 + x$  line, the gap has to close near the edge of the Brillouin zone, in order to allow the formation of a second small Fermi arc per quarter of the Brillouin zone, close to the zone edge, separated from the first one by the two hot spots. Here, this extra Fermi arc appears at dopings higher than 0.19 (see Supplemental Material).

The evolution of the Hall number depends on the parametrisation of the gap, as in any phenomenological model. The specific choices we made here correspond to the measurements on YBCO [23]. However the fact that this system goes from small Fermi arcs to a large hole pocket does not rely on fitting. Only the width of the transition can be tuned. We did not use, unlike many other parametrisation of the pseudogap, a linear dependence with respect to doping [34]. This linear dependence does not fit experimental data, even in the studies that use it. Indeed, the YRZ model with the published linear pseudogap gives  $n_H$  under the  $x$  line for  $x < 0.10$  (see Supplemental Material). This does not challenge the ability of the YRZ model to replicate experimental data, but only stresses that, there too, a linear dependence of the pseudogap in doping is inadequate.

The choice of ordering vector  $Q_0$  at the hot spots has been made according to previous studies [22]. We did however replicate the calculation for two other  $Q_0$  ordering vectors, one taken at the Brillouin zone edge, and one linking two diagonally placed hot spots. The first choice does not impact the calculations much, but the second produces an early transition of  $n_H$ , which reaches the  $1 + x$  line at  $x = 0.19$  (see Supplemental Material).

*Conclusion* — It is striking that our results fit experimental results corresponding both to transport and spectral probes closely. Indeed they agree to a remarkable extent with two types of ARPES measurements: over the Brillouin zone and resolved with respect to the  $d$ -wave factor (Figures 1 and 2, respectively). They also quanti-

tatively reproduce the evolution of the Hall number with doping (Figure 4). These results are directly inferred from the SU(2) theory of superconductors, which is derived directly from a model of antiferromagnetism with short-range coupling. This contrasts sharply with other models used to replicate these experiments, which are phenomenological theories of spin liquid states without such a strong ground. Moreover, the SU(2) theory has been shown to agree well with other experimental signatures, such as details in energy-resolved ARPES spectra [40] and in Raman scattering [39] and neutrons [41] ex-

periments. The agreement with such a wide range of experiments is indeed encouraging.

*Acknowledgments* — We would like to thank Suchitra Sebastian and Yvan Sidis for stimulating discussions. This work received financial support from the ANR project UNESCOS ANR-14-CE05-0007 and the ERC, under grant agreement AdG-694651-CHAMPAGNE. The authors also would like to thank the IIP (Natal, Brazil), where parts of this work were done, for hospitality.

- 
- [1] H. Alloul, T. Ohno, and P. Mendels, *Phys. Rev. Lett.* **63**, 1700 (1989).
  - [2] W. W. Warren, R. E. Walstedt, G. F. Brennert, R. J. Cava, R. Tycko, R. F. Bell, and G. Dabbagh, *Phys. Rev. Lett.* **62**, 1193 (1989).
  - [3] M. R. Norman and C. Pépin, *Rep. Prog. Phys.* **66**, 1547 (2003).
  - [4] E. W. Carlson, S. A. Kivelson, D. Orgad, and Emery, V. J., “Concepts in High Temperature Superconductivity,” Springer Berlin Heidelberg, Berlin, Heidelberg (2004).
  - [5] P. A. Lee, N. Nagaosa, and X.-G. Wen, *Rev. Mod. Phys.* **78**, 17 (2006).
  - [6] K. Le Hur and T. M. Rice, *Annals of Physics* **324**, 1452 (2009).
  - [7] T. M. Rice, K.-Y. Yang, and F. C. Zhang, *Rep. Prog. Phys.* **75**, 016502 (2012).
  - [8] M. R. Norman and C. Proust, *New J. Phys.* **16**, 045004 (2014).
  - [9] J. P. Carbotte, T. Timusk, and J. Hwang, *Rep. Prog. Phys.* **74**, 066501 (2011).
  - [10] M. Eschrig, *Advances in Physics* **55**, 47 (2006).
  - [11] E. Fradkin, S. A. Kivelson, and J. M. Tranquada, *Rev. Mod. Phys.* **87**, 457 (2015).
  - [12] T. Kloss, X. Montiel, V. S. de Carvalho, H. Freire, and C. Pépin, *Rep. Prog. Phys.* **79** (2016).
  - [13] A. Abanov, A. V. Chubukov, and J. Schmalian, *Adv. Phys.* **52**, 119 (2003).
  - [14] A. Chubukov, D. Pines, and J. Schmalian, in *Superconductivity*, edited by K. Bennemann and J. Ketterson (Springer Berlin Heidelberg, 2008).
  - [15] S. Sorella, G. B. Martins, F. Becca, C. Gazza, L. Capriotti, A. Parola, and E. Dagotto, *Phys. Rev. Lett.* **88**, 117002 (2002).
  - [16] E. Gull, O. Parcollet, and A. J. Millis, *Phys. Rev. Lett.* **110**, 216405 (2013).
  - [17] Z. Wang, G. Kotliar, and X.-F. Wang, *Phys. Rev. B* **42**, 8690 (1990).
  - [18] C. M. Varma, *Phys. Rev. B* **55**, 14554 (1997).
  - [19] S.-C. Zhang, *Science* **275**, 1089 (1997).
  - [20] E. Demler, W. Hanke, and S.-C. Zhang, *Rev. Mod. Phys.* **76**, 909 (2004).
  - [21] X. Montiel, T. Kloss, and C. Pépin, *arXiv:1510.03038* (2015).
  - [22] X. Montiel, T. Kloss, and C. Pépin, *Phys. Rev. B* **95**, 104510 (2017).
  - [23] S. Badoux, W. Tabis, F. Laliberté, G. Grissonnache, B. Vignolle, D. Vignolles, J. Béard, D. A. Bonn, W. N. Hardy, R. Liang, N. Doiron-Leyraud, L. Taillefer, and C. Proust, *Nature* **531**, 210 (2015).
  - [24] C. Collignon, S. Badoux, S. A. A. Afshar, B. Michon, F. Laliberté, O. Cyr-Choiniere, J. S. Zhou, S. Licciardello, S. Wiedmann, N. Doiron-Leyraud, and L. Taillefer, *arXiv:1607.05693*.
  - [25] F. Laliberté, W. Tabis, S. Badoux, B. Vignolle, D. Destraz, N. Momono, T. Kurosawa, K. Yamada, H. Takagi, N. Doiron-Leyraud, C. Proust, and L. Taillefer, *ArXiv e-prints* (2016), *arXiv:1606.04491*.
  - [26] S. Badoux, S. A. A. Afshar, B. Michon, A. Ouellet, S. Fortier, D. LeBoeuf, T. P. Croft, C. Lester, S. M. Hayden, H. Takagi, K. Yamada, D. Graf, N. Doiron-Leyraud, and L. Taillefer, *Physical Review X* **6**, 021004 (2016).
  - [27] K. M. Shen, F. Ronning, D. H. Lu, F. Baumberger, N. J. C. Ingle, W. S. Lee, W. Meevasana, Y. Kohsaka, M. Azuma, M. Takano, H. Takagi, and Z.-X. Shen, *Science* **307**, 901 (2005).
  - [28] B. Vignolle, a. Carrington, R. a. Cooper, M. M. J. French, a. P. Mackenzie, C. Jaudet, D. Vignolles, C. Proust, and N. E. Hussey, *Nature* **455**, 952 (2008).
  - [29] S. E. Sebastian, N. Harrison, and G. G. Lonzarich, *Phil. Trans. R. Soc. A* **369**, 1687 (2011).
  - [30] S. Sachdev, E. Berg, S. Chatterjee, and Y. Schattner, *Phys. Rev. B* **94**, 115147 (2016).
  - [31] V. J. Emery and S. a. Kivelson, *Nature* **374**, 434 (1995).
  - [32] A. Kanigel, U. Chatterjee, M. Randeria, M. R. Norman, G. Koren, K. Kadowaki, and J. C. Campuzano, *Phys. Rev. Lett.* **101**, 137002 (2008).
  - [33] K. Y. Yang, T. M. Rice, and F. C. Zhang, *Phys. Rev. B* **73**, 174501 (2006).
  - [34] J. G. Storey, *EPL (Europhysics Lett.)* **113**, 27003 (2016).
  - [35] S. Chatterjee, S. Sachdev, and A. Eberlein, *arXiv:1704.02329*.
  - [36] S. Caprara, M. Grilli, C. Di Castro, and G. Seibold, *J. Supercond. Nov. Magn.* **30**, 25 (2016).
  - [37] I. M. Vishik, M. Hashimoto, R.-H. He, W.-S. Lee, F. Schmitt, D. Lu, R. G. Moore, C. Zhang, W. Meevasana, T. Sasagawa, S. Uchida, K. Fujita, S. Ishida, M. Ishikado, Y. Yoshida, H. Eisaki, Z. Hussain, T. P. Devereaux, and Z.-X. Shen, *Proc. Natl. Acad. Sci.* **109**, 18332 (2012), *1209.6514*.
  - [38] K. B. Efetov, H. Meier, and C. Pépin, *Nat. Phys.* **9**, 442 (2013).
  - [39] X. Montiel, T. Kloss, C. Pépin, S. Benhabib, Y. Gallais, and A. Sacuto, *Phys. Rev. B* **93**, 024515 (2016).
  - [40] X. Montiel, T. Kloss, and C. Pépin, *EPL (Europhysics*

- Letters) **115**, 57001 (2016).
- [41] X. Montiel and C. Pépin, arXiv:1703.04442 .
- [42] P. Voruganti, A. Golubentsev, and S. John, Phys. Rev. B **45**, 13945 (1992).
- [43] A. Eberlein, W. Metzner, S. Sachdev, and H. Yamase, Phys. Rev. Lett. **117**, 187001 (2016).
- [44] G. D. Mahan, *Many-Particle Physics* (Springer, 2000).
-

# Supplemental material for: Evolution of spectral and transport quantities with doping in the SU(2) theory of cuprates

## 1. *d*-WAVE GAP

We compared the results we obtained using the SU(2) gap based on the SU(2) symmetry-breaking term to a standard *d*-wave gap used in previous studies [33, 34]

$$BM_{0,k}^2 = \left[ \frac{3t_0}{2} (0.2 - x) (\cos(k_x) - \cos(k_y)) \right]^2 \quad (\text{S1})$$

Because the dispersion of the bosonic mode is the opposite of the electronic dispersion, the gap opens everywhere but at the nodal point. Consequently, the Hall resistivity diverges at low temperature (Figure S1)

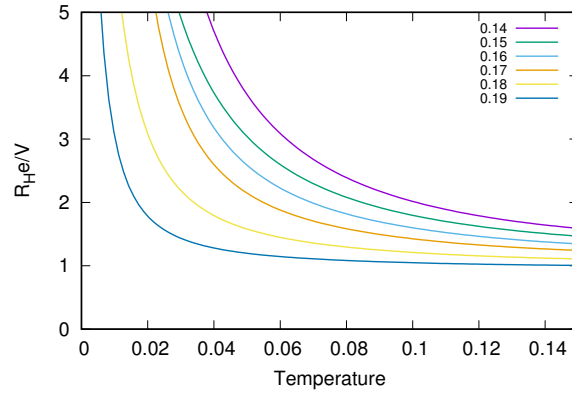


FIG. S1: Hall resistance per volume unit with respect to temperature in units of  $t_0/k_B$  for a range of hole dopings.

One can however study the evolution of the Hall number at finite temperature. Interestingly, this evolution reproduces closely the one of the Hall number extrapolated to zero temperature in the Yang-Rice-Zhang model (Figure S2).

## 2. OTHER CHOICES OF ORDERING WAVE VECTOR

Following previous work on the SU(2) theory of cuprate superconductors [22], we chose  $Q_0$  as the vector between the two closest hot spots in the main text. Here we explore the consequences of making a different choice. We used two different ordering vectors: the vector linking two points of the Fermi surface on the Brillouin zone-edge, and a diagonal vector linking two hot spots.

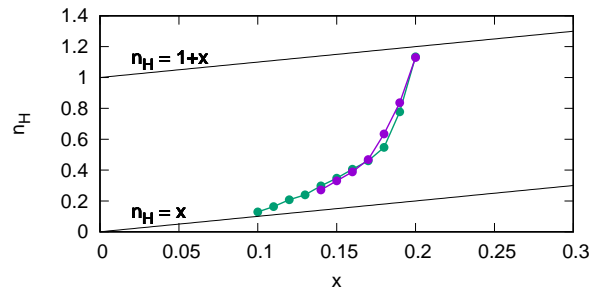


FIG. S2: Hall number at  $k_B T = 0.05 t_0 / k_B$  for a *d*-wave gap with respect to doping (purple), and Hall number at zero temperature in the Yang-Rice-Zhang model (green). The low-doping and high-doping asymptotes are also plotted for reference.



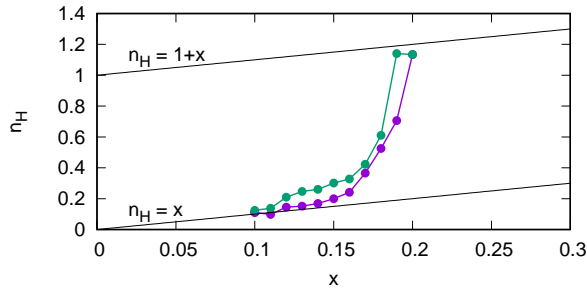


FIG. S3: Hall number with respect to doping for a zone-edge  $Q_0$  (purple), and diagonal  $Q_0$  (green). The low-doping and high-doping asymptotes are also plotted for reference.

We adjusted the gap  $\Delta_{SU2}$  in magnitude for the zone-edge  $Q_0$  vector:

$$\Delta_{SU2} = \left( \frac{1}{e^{(x-0.175) \times 170} + 1} - 0.018 \right) \times 0.61 \quad (\text{S2})$$

and for the diagonal  $Q_0$  vector

$$\Delta_{SU2} = \left( \frac{1}{e^{(x-0.175) \times 170} + 1} - 0.018 \right) \times 0.22 \quad (\text{S3})$$

Note that the only change with the gap used in the main text is the prefactor. This change is very small for the zone-edge calculation: from 0.58 to 0.61, but much larger for the diagonal  $Q_0$  vector where we use a prefactor of 0.22. A higher value of the prefactor results in  $n_H$  dropping to zero at finite doping.

The evolution of the Hall number with doping is qualitatively similar in both cases with what is found in the main text (Figure S3), except for the case of the diagonal  $Q_0$  vector very close to the critical doping. Indeed, the  $1+x$  asymptote is reached at  $x = 0.19$  already, due to the earlier closing of the gap close to the zone-edge. This is reminiscent of experiments which found similarly high Hall numbers before the closing of the pseudogap [24].

### 3. CLOSING OF THE GAP CLOSE TO THE ZONE-EDGE

Here we go back to the discussion on the case discussed in the main text, meaning longitudinal ordering wave vectors linking hot spots. As discussed in the main text, the Fermi arc opens close to the nodal point and widens when the hole doping increases. Given that the gap opens at the hot spots, it closes near the Brillouin zone edge before the transition. A second Fermi arc therefore appears, crossing the zone edge (Figure S4).

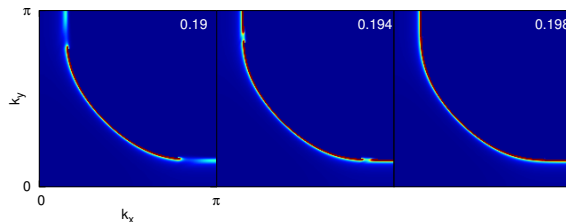


FIG. S4: Spectral function at high doping. The arising of the second Fermi arc crossing the Brillouin zone edge is clearly visible. Note that because the renormalised bands are symmetrical with respect to zero energy, both spectral functions are equal at zero frequency. We therefore only plot one of them.

### 4. COMPARISON WITH THE YRZ MODEL

We compared the doping dependence of the Hall number obtained within the  $SU(2)$  theory to the one obtained using the Yang-Rice-Zhang (YRZ) model. The dependence is similar, except that the transition is slightly sharper in our case (Figure S5).

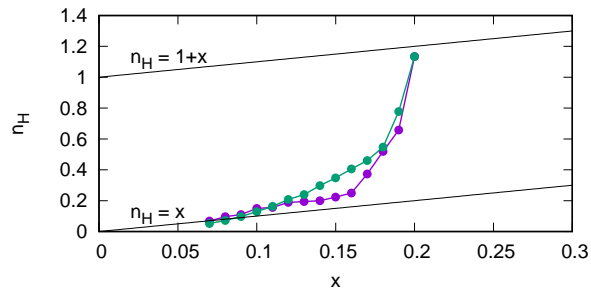


FIG. S5: Hall number with respect to doping in the SU(2) theory (purple), and Yand-Rice-Zhang (YRZ) model (green). The low-doping and high-doping asymptotes are also plotted for reference. Note that the data for the YRZ model crosses the asymptote at low doping.

We also note that the Hall number at low doping in the YRZ model is below the  $n_H = x$  line. This is due to a value of the gap which is too large. We therefore believe that describing the pseudogap by a linear function in doping is inadequate. This does not however hinder the validity of the YRZ model.